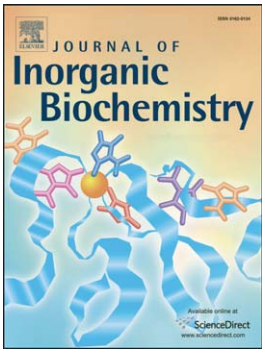

2-Nitroimidazole-ruthenium polypyridyl complex as a new conjugate for cancer treatment and visualization

Olga Mazuryk, Monika Maciuszek, Grażyna Stochel, Franck Suzenet, Małgorzata Brindell

PII: S0162-0134(14)00040-3
DOI: doi: 10.1016/j.jinorgbio.2014.02.001
Reference: JIB 9467

To appear in: *Journal of Inorganic Biochemistry*

Received date: 15 July 2013
Revised date: 2 February 2014
Accepted date: 2 February 2014

Please cite this article as: Olga Mazuryk, Monika Maciuszek, Grażyna Stochel, Franck Suzenet, Małgorzata Brindell, 2-Nitroimidazole-ruthenium polypyridyl complex as a new conjugate for cancer treatment and visualization, *Journal of Inorganic Biochemistry* (2014), doi: 10.1016/j.jinorgbio.2014.02.001

2-Nitroimidazole-ruthenium polypyridyl complex as a new conjugate for cancer treatment and visualization

Olga Mazuryk[a,#], Monika Maciuszek[a,b,#], Grażyna Stochel[a], Franck Suzenet[b,*], Małgorzata Brindell[a,*]

[a] *Department of Inorganic Chemistry, Faculty of Chemistry, Jagiellonian University, Ingardena 3, 30-060 Krakow, Poland*

[b] *Institut of Organic and Analytical Chemistry, University of Orléans, UMR-CNRS 7311, rue de Chartres, BP 6759, 45067 Orléans Cedex 2, France*

*Corresponding authors:

Dr. Małgorzata Brindell

Faculty of Chemistry

Jagiellonian University

Ingardena 3, 30-060 Krakow, Poland

brindell@chemia.uj.edu.pl

phone: +48126632221

fax: +48126340515

Dr. Franck Suzenet

Institut de Chimie Organique et Analytique

UMR-CNRS 7311, Université d'Orléans

rue de Chartres, 45067 Orléans, France

franck.suzenet@univ-orleans.fr

phone: +33238494580

fax: +33238417281

[#]Both authors contributed equally as the first co-authors.

Abstract

A novel long-lifetime highly luminescent ruthenium polypyridyl complex containing 2-nitroimidazole moiety $[Ru(dip)_2(bpy\text{-}2\text{-}nitroIm)]Cl_2$ (dip = 4,7-diphenyl-1,10-phenanthroline, bpy-2-nitroIm = 4-[3-(2-nitro-1H-imidazol-1-yl)propyl]-2,2'-bipyridine) has been designed cancer treatment and imaging. The luminescence properties of the synthesized compound strongly depend on the oxygen concentration. Under oxygen-free conditions quantum yield of luminescence and the average lifetime of emission were found to be 0.034 and 1.9 μs, respectively, which is ca. three times higher in comparison to values obtained in air-equilibrated solution. The binding properties of the investigated ruthenium complex to human serum albumin have been studied and the apparent binding constant for the formation of the protein-ruthenium adduct was determined to be 1.1×10^5 M^{-1}. The quantum yield and the average lifetime of emission are greatly enhanced upon binding of ruthenium compound to the protein. The DNA binding studies revealed two distinguished binding modes which lead to a decrease in luminescence intensity of ruthenium complex up to 60% for [DNA]/[Ru] < 2, and enhancement of emission for [DNA]/[Ru] > 80. Preliminary biological studies confirmed fast and efficient accumulation of the ruthenium complex inside cells. Furthermore, the ruthenium complex was found to be relatively cytotoxic with LD_{50} of 12 and 13 μM for A549 and CT26 cell lines, respectively, under normoxic conditions. The retention and cellular uptake of ruthenium complex is enhanced under hypoxic conditions and its LD_{50} decreases to 8 μM for A549 cell line.

Keywords: ruthenium polypyridyl complex, theranostic, cytotoxicity, optical imaging, luminescence, DNA

1. Introduction

Recently a new approach based on combining of diagnostic and therapeutic properties in one compound or platform (in case of nanoparticles) so called theranostics has attracted interest of researchers [1, 2]. Such strategy offers many advantages over classical one, among others the real-time monitoring of the therapeutic effect which can help to optimize the treatment schedule for each patient individually. Moreover, the visualization of drug biodistribution and its accumulation allow for better protection of healthy tissues by the controlling drug administration as well as using protective agents.

Polypyridyl ruthenium complexes are very interesting class of compounds which by a proper designing can combine properties needed for the treatment of the cancer as well its visualization. The unique optical features (intense and long lifetime luminescence strongly depending on the molecular oxygen concentration, emission close to near-infrared) together with favorable biological properties (ability to pass cellular membrane, reasonable solubility in aqueous media) give rise to their application in an optical imaging. They can be applied as probes not only for the fluorescence molecular tomography (FMT) but also for the fluorescence lifetime imaging microscopy (FLIM), where the signal-to-background ratios can be significantly improved by suppressing short-lived autofluorescence. Recently, a series of phosphorescent ruthenium-complexes of the type $[Ru(bpy)_2L]^{2+}$, where L is phenanthroline ligand modified by hydrophobic substituents (an alkyl side chain or an aromatic hydrocarbon) have been employed for non-invasive imaging of physiological hypoxia in living organism [5]. It is well-known, that state of hypoxia is a consequence of chaotic and poor vascular organization in the tumor leading to lower efficiency in delivering of oxygen and nutrition. Moreover, it is suggested that hypoxia causes resistance to standard therapies and promotes a more malignant phenotype [6]. Therefore, the targeting of cancer cells by using the hypoxia state as a unique feature of solid tumors seems to be very attractive [7].

Lately several research groups have taken an advantage of photophysical properties of polypyridyl ruthenium complexes and functionalized them with different moieties such as porphyrins (photodynamic therapy) [8], coumarins (esterase sensing) [9], estradiols (targeting estrogen receptor-α ER- α) [10], squalene (cellular imaging tool) [11] and short peptides (targeting the nucleus) [12, 13]. The aim of our study was to modify of polypyridyl ruthenium complexes to increase cellular accumulation, to obtain better selectivity toward hypoxic tissues as well as to combine cytotoxic activity with imaging properties. Several recent studies have shown that the ruthenium complexes comprising two 4,7-diphenyl-1,10-phenantroline (dip) ligands exhibits better uptake by cells over complexes with simple bpy or phen ligands [14, 15]. This feature encourages us to use $[Ru(dip)_2L]^{2+}$ platform for designing of new complexes.

2-Nitroimidazoles are the group of bioreductive prodrugs which are developed toward their application in diagnosis and therapy of hypoxic tissues characteristic for tumors [16]. Pimonidazole (α-((2-nitroimidazol-1-yl)methyl)-1-piperidineethanol) has been commonly applied for the detection and quantification of hypoxia [16, 17] and currently is studied as an invasive hypoxia diagnostic tool for pancreatic tumor in a pre-operation treatment [18]. This approach is limited by the requirements for biopsy of the tissue followed by the complex immunohistochemical test. To overcome this problem the hypoxic tracer can be labeled with radionuclides, the most often ^{18}F for PET imaging [7]. Alternatively, 2-nitroimidazole moiety can be attached to the another unit responsible for imaging. The first attempts to obtain the near-infrared fluorescent probes for imaging of tumor hypoxia by combining of 2-nitroimidazole moiety with NIR fluorophore (indocyanine green, tricarbocyanine) have been recently reported and tested *in vivo* [23, 24].

In view of the recent findings we report the synthesis of a new agent for cancer treatment and its visualization based on ruthenium polypyridyl complex and 2-nitroimidazole

as depicted in Scheme 1. The synthesis, photophysical, protein/DNA-binding and biological properties of $[Ru(dip)_2(bpy\text{-}2\text{-}nitroIm)]^{2+}$ are discussed in the context of its potential use in anticancer therapy combine with visualization of cancer tissue.

Scheme 1

2. Materials and methods

*2.1. **Synthetic procedures***

Materials and general procedures are described in supplementary information. *2,2'-Bipyridyl-1-oxide* (**2**), *4-nitro-2,2'-bipyridyl-1-oxide* (**3**) and *4-bromo-2,2'-bipyridine* (**4**) were prepared according to published procedures [25].

*2.1.1. 3-(2,2'-bipyridin-4-yl)prop-2-yn-1-ol (**5**)*

In a sealed tube under argon atmosphere 4-bromo-2,2'-bipyridine (**4**, 0.05 g, 0.23 mmol) and propargyl alcohol (0.019 g, 0.35 mmol, 0.02 mL, 1.5 eq) were added to 2.5 mL of anhydrous DME. To the reaction mixture 1.5 mL of triethylamine was added and the solution was degassed. Finally $Pd(PPh_3)_4$ (0.0129 g, 0.011 mmol, 0.05eq) was added. The mixture was heated to 120 °C for 3 h under microwave irradiations. After cooling down, solution was filtrated on the celite. Filtrate was evaporated and crude product was dissolved in the small amount of acetone. Then, under vigorous stirring diethyl ether and next hexane were added to allow triphenylphosphine derivative to precipitate. Mixture was filtrated on a Büchner funnel over a large plug of silica and washed with diethyl ether and hexane. The filtrate was evaporated under reduced pressure to afford the final product as a yellowish solid in 56% yield. IR (cm^{-1}): 664, 787, 853, 905, 973, 993, 1034, 1088, 1213, 1391, 1461, 1538, 1566, 1581, 1601, 2850, 2914, 3031, 3217. ^{1}H-NMR (400 MHz, $CDCl_3$): δ/ppm = 2.19-2.12 (1H, t),

4.53 (2H, d, J = 6.2 Hz), 7.28 (1H, dd, J = 5.0, 1.4Hz), 7.36 (1H, m) 7.87-7.79 (1H, m), 8.38 (1H, dd, J = 8.0, 1.0 Hz), 8.44 (1H, s), 8.63 (1H, d), 8.68(1H, dd, J = 3.5, 1.3 Hz); ^{13}C NMR (101 MHz, $CDCl_3$) δ/ppm = 156.25, 155.41, 149.15, 149.23, 137.02, 131.78, 125.35, 124.03, 123.30, 121.17, 92.01, 83.38, 51.44. HRMS $[M+H]^+$ *m/z* calculated for $C_{13}H_{11}N_2O$: 211.2319; found: 211.0868.

*2.1.2. 4-(3-hydroxypropyl)-2,2'-bipyridine (**6**)*

3-(2,2'-Bipyridin-4-yl)prop-2-yn-1-ol (**5**, 150 mg) was dissolved in 25 mL of ethanol and the solution was degassed with argon. Pd/C (0.030 g) was added and reaction mixture was bubbled with hydrogen. Reaction was stirred at room temperature for 3 h under H_2 atmosphere. The solution was filtrated on celite and concentrated under reduced pressure to obtain an oily residue. Purification through a short column chromatography on silica gel afforded the desired product as a creamy oil in 98% yield. ^{1}H NMR (400 MHz, $CDCl_3$) δ 8.67 (d, 1H), 8.56 (dd, *J* = 4.8, 2.7 Hz, 1H), 8.39 (d, *J* = 8.0 Hz, 1H), 8.24 (s, 1H), 7.82 (t, *J* = 6.8 Hz, 1H), 7.34 – 7.27 (m, 1H), 7.16 (s, 1H), 3.69 (s, 2H), 2.81 (t, *J* = 8.9 Hz, 2H), 2.46 (s, 1H), 2.02 – 1.91 (p, *J* = 9.3 Hz, 2H). ^{13}C-NMR (400 MHz, $CDCl_3$): δ/ppm = 156.22, 155.99, 152.06, 149.03, 137.04, 127.81, 123.71, 121.36, 121.31, 61.58, 33.03, 31.59. HRMS $[M+H]^+$ *m/z* calculated for $C_{13}H_{15}N_2O$: 215.2716; found: 215.1180.

*2.1.3. 4-(3-bromopropyl)-2,2'-bipyridine (**7**)*

130 mg of 4-(3-hydroxypropyl)-2,2'-bipyridine (**6**) was dissolved in 2.4 mL of a 1:1 mixture of HBr (33% in acetic acid) and water. The reaction mixture was then heated to reflux overnight. After cooling down to room temperature, a saturated aqueous solution of sodium bicarbonate was added until the pH reached 5-6. The aqueous phase was extracted three times with dichloromethane (3 × 10 mL). Organic phases were dried over $MgSO_4$, filtered and

evaporated under reduce pressure. Purification on a short aluminia column with DCM/Petroleum ether (8/2) as eluent afforded compound 7 as a pink-orange oil in 50% yield. ^{1}H-NMR (400 MHz, $CDCl_3$): δ/ppm = 8.67 (1H, dd, J 4.8, 8 Hz), 8.56 (1H, dd, J 10.9, 5.0 Hz), 8.41-8.35 (1H, m), 8.26 (1H, s), 7.85-7.75 (1H, m), 7.30 (1H, dt, J =1 0.9, 4.8Hz), 7.16 (1H, d, J = 4.9 Hz), 3.42 (2H, t, J = 6.7 Hz), 2.87 (2H, t, J = 7.5 Hz), 2.31-2.20 (2H, m). ^{13}C NMR (101 MHz, $CDCl_3$) δ 156.28, 156.09, 150.57, 149.32, 149.11, 136.96, 124.05, 123.75, 121.24, 121.07, 33.61, 33.00, 32.62. HRMS $[M+H]^+$ *m/z* calculated for $C_{13}H_{14}{}^{79}BrN_2$: 277.08; found: 277.0338.

*2.1.4. 4-[3-(2-nitro-1H-imidazol-1-yl)propyl]-2,2'-bipyridine (**8**, bpy-2-nitroIm)*

2-Nitroimidazole (0.033 g, 1 eq), potassium carbonate (1 eq) and 4-[3-(bromopropyl]-2,2'-bipyridine (**7**, 0.08g) were dissolved in 2 mL of dry DMF. The mixture was heated at 110°C for 3 hours under argon atmosphere. After cooling down to room temperature, most of the DMF was evaporated under the reduced pressure and the residue was dissolved in AcOEt (10 mL) and washed 3 times with water (3 x 10mL). Organic layer was dried over magnesium sulfate, filtrated and evaporated under reduced pressure. Crude product was washed with ice-cold n-pentane and filtrated on Millipore apparatus. The resulting pinkish solid was isolated in 35% yield and used without any further purification. The melting point was found in the range 104-106 °C. IR (cm^{-1}): 3123, 1599, 1583, 1557, 1456, 1284, 1244, 1179, 1122, 1092, 991, 856, 759, 636. ^{1}H NMR (400 MHz, $CDCl_3$) δ 8.67 (dd, *J* = 3.9, 0.8 Hz, 1H), 8.60 (t, *J* = 4.2 Hz, 1H), 8.41 (d, *J* = 8.0 Hz, 1H), 8.25 (s, 1H), 7.82 (td, *J* = 7.8, 1.8 Hz, 1H), 7.32 (ddd, *J* = 7.4, 4.7, 1.1 Hz, 1H), 7.15 (s, 1H), 7.14 (s, 1H), 7.06 (d, *J* = 3.1 Hz, 1H), 4.46 (dd, *J* = 12.9, 5.6 Hz, 2H), 2.84 – 2.74 (t, 2H), 2.36 – 2.24 (p, 2H). ^{13}C NMR (101 MHz, $CDCl_3$) δ 156.47, 155.86, 149.72, 149.53, 149.12, 137.03, 128.57, 125.77, 123.90, 123.60, 121.26, 120.72,

49.60, 32.07, 30.78. HRMS $[M+H]^+$ *m/z* calculated for $C_{16}H_{16}N_5O_2$: 310.3313; found: 310.1297.

2.1.5. [Ru(dip)$_2$(bpy-2-nitroIm)]Cl$_2$

The synthetic procedure was adapted from the literature [26]. In the round-bottomed flask $Ru(dip)_2Cl_2 \bullet DMF \bullet H_2O$ (52 mg, 0.06 mmol, 0.92 eq, synthesized according to literature procedure[26]), NaOAc (13.5 mg, 0.1625 mmol, 2.5 eq) and bpy-2-nitroIm (20 mg, 0.065 mmol, 1 eq) were dissolved in a methanol/water mixture (25 mL, 4/1 v/v). The solution was heated to reflux for 31 h. The reaction mixture was then cooled to rt, and concentrated to one-third by evaporation of the solvent. Brine was added to the mixture, and the resulting precipitate was filtered. The solid was dissolved in methanol and the solution was filtrated. Filtrate was evaporated and residue was dissolved in a small volume of dichloromethane. Toluene was then added slowly to the filtrate and a new precipitation occurred. The product was filtrated and isolated as an orange solid. The resulting filtrate was treated as the previous one and more product was obtained after the solution was left standing at 4 °C for a few days. Solids were combined and dried under vacuum to give the final product (50 mg, 72%) as a microcrystalline dark orange powder. IR (cm^{-1}) = 3360, 3055, 1619, 1556, 1478, 1440, 1415, 1357, 1080, 834, 766, 737, 702 HRMS $[M]^{2+}$ *m/z* calculated for $[C_{64}H_{47}N_9O_2Ru]^{2+}$ 537.6451 found: 537.6450 (see Fig. S1) The purity of the obtained compound was further checked by TLC (all types mentioned in the general part) as well as HPLC analysis (see Fig. S2).

2.2. *Spectroscopic measurements*

UV–visible absorption spectra were recorded on a Perkin Elmer Lambda 35 spectrophotometer using quartz cells with a 1-cm optical pathlength. Optical properties were

examined in aqueous solutions containing DMSO (<0.04% v/v). Luminescence measurements were performed on a spectrofluorimeter Perkin Elmer LS55 in a quartz cell with a 1-cm pathlength. The spectra were recorded at the room temperature in aqueous solution containing small amount of DMSO (<0.008% v/v). The emission spectra were recorded between 470 and 860 nm upon excitation at 463 nm. The average of three scans was subjected to smoothing. For determination of the quantum yield of luminescence (Φ), aqueous solutions of $[Ru(bpy)_3]^{2+}$ with a small amount of DMSO (<0.008% v/v) were used as standards (Φ = 0.028 [27] and 0.042 [28] for air-equilibrium and deoxygenated conditions, respectively). The spectra were recorded at the concentration less than 0.05 absorbance unit at the excitation wavelength. Values were calculated according to the following equation [4]:

$$\boldsymbol{\Phi = \Phi_{ref} \times [A_{ref}/A] \times [I/I_{ref}] \times [n^2/n_{ref}^2]}$$

where ***I*** is the integrated intensity of luminescence, ***A*** is the optical density, and ***n*** is the refractive index, ***ref*** refers to the values for reference. The mean value from minimum three independent experiments was calculated.

The luminescence lifetime measurements were performed with a single photon counting technique using Fluorolog-3, Horiba Jobin Yvon. The excitation wavelength was set at 464 nm (NanoLed Diodes) and the average lifetime of luminescence was monitored at 621 nm. Luminescence decays were collected with 1000 counts in the peak. The instrument response functions were measured using a light scattering solution of Ludox (colloidal silica, Sigma-Aldrich). Experiments were conducted at room temperature. The DAS6 software (HORIBA Scientific) was used for deconvolution of the obtained decays and for calculation of the lifetime values. The quality of the fit was judged by the χ^2 parameter (the goodness of fit evaluation). One-exponential fit was determined to be an optimal description of the obtained results for the free compound; but after binding with protein and DNA single-

exponential decay was not efficient and two-exponential fit was modeled (similar as in reference [29]).

2.3. Protein and DNA-binding studies

The protein solution was prepared by dissolving of human serum albumin (HSA) in water and its concentration was determined spectrophotometrically from the molar absorptivity of 4.4×10^4 cm^{-1} M^{-1} at 280 nm [30]. The quantum yield of luminescence for ruthenium complex in the present of HSA (1 μM) was measured using the same procedure as described for ruthenium complex alone.

Calf thymus deoxyribonucleic acid was purchased from Sigma-Aldrich and its stock solution was prepared by dissolving of solid DNA in water. DNA concentrations per nucleotide were determined by absorption spectroscopy using the molar absorption coefficient of 6600 $M^{-1}cm^{-1}$ at the wavelength of 260 nm. DNA binding experiments were performed in 0.05 M Tris/HCl buffer (pH 7.4) at 37 °C. The emission titration studies were performed by using fixed concentration of ruthenium compound (3 μM). The DNA aliquots were added and after 5 min of incubation fluorescence spectra upon excitation of 463 nm were measured. The average of three scans was subjected to smoothing and the fluorescence intensities were corrected due to dilution effects.

2.4. Biological studies

For biological evaluation murine colon carcinoma cell line (CT26) as well as human lung adenocarcinoma epithelial cell line (A549) were used. Cells were cultured in DMEM medium supplemented with ferine serum (10%) and antibiotics (1%) – penicillin (100 units/mL) and streptomycin (100 μg/mL) at atmosphere of 5% CO_2 at 37 °C. For hypoxia treatments, cells were placed in a humidified atmosphere containing 94% N_2, 5% CO_2 and 1% O_2 gas mixture in hypoxic station Whitley H35. Cells and medium intended for hypoxic experiments were preincubated at hypoxic chamber for 24 h. The evaluation of accumulation

of $[Ru(dip)_2(bpy\text{-}2\text{-}nitroIm)]Cl_2$ in CT26 cells under normoxic conditions was conducted using 96 wells plates with the seeding density of cell at 30 000 cells per well. Cells were cultivated for 2 days, then the medium was washed out and dissolved ruthenium compound was added into the wells. $[Ru(dip)_2(bpy\text{-}2\text{-}nitroIm)]Cl_2$ was dissolved in DMSO and diluted in PBS with Ca^{2+}/Mg^{2+} to the required concentration ($0\text{-}50 \times 10^{-6}$ M) immediately prior to addition into the wells. The PBS buffer was used to avoid interaction of the ruthenium complex with medium ingredients due to a high lipophilicity of the compound. The final DMSO concentration was kept at 0.5% v/v level, since this amount of DMSO does not influence cells viability (LD_{50} for aqueous solution of DMSO was found to be of 5 μM, results not shown). Compound was incubated with the cells for 4 and 24 hours and then was washed out. Cells were washed with PBS buffer (with Ca^{2+}/Mg^{2+}) and were kept in PBS for further studies. The luminescence measurements were recorded using Infinite 200 microplate reader (Tecan) with 463 nm as an excitation wavelength and 621 nm as an emission wavelength. Each well was measured at 25 points and the mean value was calculated.

Cellular uptake for A549 cells under both normoxic and hypoxic conditions was monitored by flow cytometry. A549 cells were seeded on a 24 well plates with a density 35 000 cells per well. 24 h after the seeding $[Ru(dip)_2(bpy\text{-}NitroIm)]^{2+}$ and $[Ru(dip)_2(bpy)]^{2+}$ were added at 2, 4 and 6 μM concentrations. Cells were incubated in medium without and with serum (2% FBS) under hypoxic and normoxic conditions for 24 h. After incubation, cells were washed twice with PBS, trypsinisized and analyzed by LSRII cytometer (Becton Dickinson) with λ_{ext} at 488 nm and λ_{em} at 610 ± 10 nm. Experiment was analyzed using BD FACSDiva Software. 10 000 singular gated events were collected. Moreover, the ability of ruthenium compounds to retain in cells under hypoxic conditions was assessed also after 24 h of cell cultivation in medium not supplemented with these complexes. After 24 h of incubation with $[Ru(dip)_2(bpy\text{-}NitroIm)]^{2+}$ and $[Ru(dip)_2(bpy)]^{2+}$ (2, 4 and 6 μM, diluted in

DMEM with 2 % FBS), cells were washed twice with PBS, trypsinisized and the first half of cells was analyzed by flow cytometry. Another half was seeded on the new well, fresh medium was applied, and cells remained under hypoxic conditions for another 24 h, followed by trypsinisization and analyzing by flow cytometry.

The cytotoxicity studies on CT26 cells were performed using MTT test [31]. Cells were cultivated in 96 wells plates for a day prior to addition of the investigated compounds. After 4 or 24 h incubation of the CT26 cells either with ligand alone (bpy-2-nitroIm, **8**) or the investigated ruthenium complex in the PBS solution were washed out and subsequently 200 µl of fresh medium was applied to allow cells repair existed damages. After 24 h, the medium was replaced with 3-(4,5-dimethylthiazol-2-yl)-2,5-diphenyltetrazolium bromide salt (MTT) dissolved in DMEM (0.5 mg/ml) to determine the cell viability. After 3 h of incubation the MTT solution was washed out and crystals were dissolved in methanol:DMSO at volume ratio of 1:1. Then the absorbance value at 565 nm was recorded using Infinite 200 microplate reader (Tecan). Three series of minimum two plates were performed and SD of a mean value was calculated.

The evaluation of the cytotoxicity of $[Ru(dip)_2(bpy\text{-}2\text{-}nitroIm)]^+$ on A549 cells was conducted using Alamar Blue assay. The ruthenium complex dissolved in medium (DMSO 0.1 %) was incubated with the cells for 24 h under hypoxia or normoxia conditions and then was washed out. Cells were washed with PBS buffer (with Ca^{2+}/Mg^{2+}) and resazurin sodium salt (25 10^{-6} M) diluted in PBS was added to the wells. The fluorescence measurements were recorded using Infinite 200 microplate reader (Tecan) with λ_{ext} at 565 nm and λ_{em} at 605 nm. Each well was measured at 25 points and the mean value was calculated. Experiments were repeated three times in triplicates. The viability was calculated with regard to the untreated cells control. The LC_{50} values were determined using Hill equation (Origin 9.0) [31].

$$y = y_0 + \frac{(y_{100} - y_0)[c]^H}{[IC_{50}]^H + [c]^H}$$

For cell imaging Olympus fluorescence microscope IX51 equipped with XC10 camera was used. Cells were seeded into round dishes with density 300 000 cells/dish. After cultivation for 24 h cells were incubated with different concentration of $[Ru(dip)_2(bpy\text{-}2\text{-}nitroIm)]Cl_2$ (0, 0.5, 1, 5 and 10 μM). The ruthenium complex was dissolved in PBS buffer with Ca^{2+}/Mg^{2+} with small amount of DMSO (0.5% v/v). After incubation (1 h, 37 °C) ruthenium compound was washed out and cells were washed with PBS three times. Next, keeping cells in PBS buffer, images of $[Ru(dip)_2(bpy\text{-}2\text{-}nitroIm)]Cl_2$ embedded in CT26 cells were taken using 470-495 nm excitation filter.

3. Results and discussion

3.1. Synthesis

The synthesized complex is composed of ruthenium polypyridyl moiety as the luminescent dye with the 2-nitroimidazole moiety attached with alkyl spacer to the bipyridyl ligand as a potential hypoxia sensitive unit. The overview of the synthetic pathway is presented in Scheme 2. 4-Bromo-2,2'-bipyridine (**4**) was obtained from commercially available 2,2'-bipyridine in a three steps sequence [25, 32, 33]. A Sonogashira cross-coupling reaction with propargylic alcohol under microwaves activation afforded the alkyne intermediate (**5**). After hydrogenation and reaction with hydrobromic acid, the bromopropylbipyridine (**7**) was reacted with 2-nitroimidazole to afford the desired bpy-2-nitroIm (**8**). The $Ru(dip)_2Cl_2$ synthesized according to published procedure [26] was reacted with (**8**) in methanol/water mixture (4/1 v/v) following literature method developed for the substitution with monocarboxylic bipyridyl ligand [26]. Purity and identity of the final compound $[Ru(dip)_2(bpy\text{-}2\text{-}nitroIm)]Cl_2$ was confirmed by the presence of single peak in

HPLC chromatogram and in high resolution mass spectrum with *m*/*z* = 537.6450 for $[C_6H_{47}N_9O_2Ru]^{2+}$ (see Supplementary material Fig. S1 and S2).

Scheme 2

3.2. Photophysical characterization

Due to quite satisfactory solubility of the compound in water, all photophysical properties were measured in aqueous solution with a small addition of DMSO (<0.04%). The absorption spectrum of $[Ru(dip)_2(bpy\text{-}2\text{-}nitroIm)]^{2+}$ is shown in Fig. 1. The narrow and intense band at 278 nm (ε = 88 400 ± 100 $M^{-1}cm^{-1}$) have been assigned to a spin allowed ^{1}LC ($^1\pi\rightarrow\pi^*$ bpy-centered) transition [34]. The shoulder at 314 nm (ε = 25 900 ± 100 $M^{-1}cm^{-1}$) originates from a ^{1}LC transition of phenanthroline moiety. At visible region of spectrum two bands at 433 nm (ε = 19 100 ± 100 $M^{-1}cm^{-1}$) and 463 nm (ε = 19 700 ± 100 $M^{-1}cm^{-1}$) are attributed to the spin allowed ^{1}MLCT $d\rightarrow\pi^*$ transitions (assignment based on [34]). New synthesized ruthenium complex was found to be luminescent in aqueous solution with the emission maximum occurring at 621 nm (excitation at 463 nm). A very large Stoke's shift of 150 nm is observed, which is not encounter for NIR organic dyes proposed as selective fluorescent probe for hypoxia [23, 24].

Fig. 1.

The quantum yield of luminescence of the studied complex was determined in aqueous solution at room temperature both in air equilibrated (Φ_{air} = 0.010 ± 0.0004) and deoxygenated solution (Φ_{Ar} = 0.034 ± 0.0004). The increased quantum yield in oxygen-free

solution is an important feature since the synthesized complex is designed for imaging of cancer tissues which very often exhibit lower oxygen concentration. Average emission lifetime for $[Ru(dip)_2(bpy\text{-}2\text{-}nitroIm)]^{2+}$ in air-equilibrated water solution was found to be 700 ± 10 ns (660 ± 10 in TRIS buffer, pH 7.4) suggesting that the emission takes place from triplet sate, typically found for these type of ruthenium complexes. In the oxygen-free solution emission lifetime dramatically increases up to 1.9 ± 0.1 μs, that makes $[Ru(dip)_2(bpy\text{-}2\text{-}nitroIm)]^{2+}$ an interesting candidate for luminescence reporter for monitoring the oxygen concentration using fluorescence lifetime imaging microscopy. Moreover, the compound is very stable in aqueous solution as confirmed by the absence of changes in the absorption and emission spectra during at least 24 h. Sufficient solubility in water, high molar absorptivity together with the increased yield of luminescence and average lifetime in oxygen-free solution create a strong opportunity to use of $[Ru(dip)_2(bpy\text{-}2\text{-}nitroIm)]^{2+}$ as luminescent probe for imaging cancer cells.

3.3. Reactivity towards biomacromolecules (human serum albumin and calf thymus DNA)

3.3.1. Enhancement of ruthenium complex luminescence in the presence of human serum albumin

The interaction of $[Ru(dip)_2(bpy\text{-}2\text{-}nitroIm)]^{2+}$ with human serum albumin (HSA) was found to be a moderate with an association constant for the formation of HSA-Ru-complex adducts ca. 10^5 M^{-1} (more details concerning this experiment are available in Supplementary Information). This correlates very well with association constants calculated for other ruthenium polypyridyl complexes [35]. The binding of $[Ru(dip)_2(bpy\text{-}2\text{-}nitroIm)]^{2+}$ to HSA also effect its luminescence spectra leading to gradual increase of the emission intensity and

shift of the maximum toward shorter wavelengths (Fig. S4, experimental details are described in Supplementary Information). The observed increase for both the luminescence quantum yield as well as the average lifetime of emission is dependent on protein concentration as shown in Fig. 2. It is very likely that the interaction of $[Ru(dip)_2(bpy\text{-}2\text{-}nitroIm)]^{2+}$ with HSA leads to spatial separation of nitroimidazole moiety from Ru center by protein scaffold. In this way protein can prevent from quenching its luminescence by this residue. It can be assumed that if such interaction occurs inside the cells also with another proteins, the enhancement of the luminescence should be manifested. Taking into account increased amount of the proteins inside cells (50 – 400 mg/ml) [36] this feature is very interesting in the context of application of $[Ru(dip)_2(bpy\text{-}2\text{-}nitroIm)]^{2+}$ as potential cellular dye. Previously, reported increased photoluminescence lifetimes for ruthenium compound $[Ru(bpy)_2(5\text{-}iodoacetamido\text{-}1,10\text{-}phenantroline)](PF_6)_2$ from 490 ns for free complex to 809 and 895 ns after covalent binding with human serum albumin and human immunoglobulin G, respectively, have been also reported [29].

Fig. 2.

3.3.2. Unusual effect of calf thymus DNA on luminescence of ruthenium complex

DNA-binding ability of $[Ru(dip)_2(bpy\text{-}2\text{-}nitroIm)]^{2+}$ is rather moderate (ca. 5.0×10^5 M^{-1}, for details see Supplementary Information) in comparison to classical intercalators $[Ru(bpy)_2(dppz)]^{2+}$ (3.1×10^6 M^{-1}) or $[Ru(phen)_2(dppz)]^{2+}$ (5.1×10^6 M^{-1}) [37]. These and the other typical intercalators after addition of the DNA show a substantial increase of luminescence [38] which can arise either from the protection of the ruthenium complex from quenching by water molecules by the hydrophobic environment inside the DNA or by the reduction of the complex mobility leading to the decrease of the vibration mode of relaxation [43]. In contrast for the studied ruthenium complex the small excess of the DNA ([DNA]/[Ru]

≤ 10) results in decreases of luminescence intensity down to 65 % (Fig. S7A). Slight decrease of the average lifetime of luminescence is also observed from $\tau_{unbound}$ = 660 ± 10 ns to a τ_{bound} = 540 ± 10 ns for [DNA]/[Ru] ratio = 10. The Stern-Volmer analysis shows that K_{sv} equals 1.96×10^4 M^{-1}, and taking into account the lifetime of luminescence for ruthenium complex (τ_0 = 660 ± 10 ns in TRIS/HCl buffer), the bimolecular quenching constant k_q is 3.0×10^{10} M^{-1} s^{-1}. Such value suggests that the observed quenching comes probably from diffusion interaction between the DNA and ruthenium complex and/or weak binding interaction between molecules [4]. This weak binding is accompanying by electrostatic interaction as confirmed by the observed quicker quenching of luminescence in water than in the buffer solution for [DNA]/[Ru] < 10. The presence of surface interaction is typically found for such systems since ruthenium complexes possess positive charge (2+) [44].

Addition of higher excess of the DNA up to [DNA]/[Ru] ratio of 80 does not cause any changes in luminescence spectra of the ruthenium complex. However, further increased in the DNA concentration leads to recovery of the luminescent properties by ruthenium complex and even the enhancement of the emission at large DNA excess (Fig. S7B). A small hypsochromic shift of emission maximum ca. 2 nm is observed. Increased the average lifetime of luminescence is also detected from $\tau_{unbound}$ = 660 ± 10 ns to a τ_{bound} = 1.24 ± 0.02 μs for [DNA]/[Ru] ratio = 200. The increased in ruthenium complex luminescence and average lifetime of luminescence is observed only at very high concentration of the DNA, unlike as for other intercalative and major groove binding ruthenium complexes for which [DNA]/[Ru] ratio of 1 is usually enough for the substantial luminescence intensification [38, 41, 45, 46]. Interestingly, ruthenium compound in the presence of high concentration of the DNA promotes the DNA condensation possibly after its structure distortion. This type of interaction is often observed for the polyamines interacting with DNA [42]. The packing of the DNA around the ruthenium complex changes its environment into more rigid and less

polar one. Entrapment of ruthenium complex in such matrix results in the hypsochromic shift of emission peak as well as the increase of luminescence intensity. Similar photophysical behavior is observed for the $[Ru(bpy)_3]^{2+}$ assembled into sol-gel materials [47]. The aggregation of the complex on the DNA template has been reported for mixed ligand ruthenium(II) complexes with 5,6-dimethyl-1,10-phenantroline [48].

Ruthenium(II) complexes with polypyridyl ligands can interact with the DNA in several noncovalent modes such as electrostatic binding, groove binding or intercalation [49]. $[Ru(dip)_2(bpy\text{-}2\text{-}nitroIm)]^{2+}$ interacts with DNA at least in two different ways. On small excess of the DNA the ruthenium complex exhibits tight interaction with helix, probably by partial intercalation or groove binding, as it is confirmed by UV-visible and luminescence titration and ethidium bromide competitive binding experiment (more details concerning these experiments are available in Supplementary Information). At higher excess of the DNA the additional interaction takes place (probably strong hydrophobic interaction with the DNA surface) as it is confirmed by the increased intensity of luminescence of ruthenium compound. The classical intercalation binding mode can be excluded as shown by the thermal denaturation studies (compare the Supplementary Information).

3.5. Preliminary cellular studies – normoxic conditions

Evaluation of biological properties of $[Ru(dip)_2(bpy\text{-}2\text{-}nitroIm)]^{2+}$ was conducted on CT26 mouse carcinoma cells. The uptake of this complex was investigated by taking an advantage of its luminescence properties using microplates reader for the quantification of its internalization as well as microscopy imaging for the assessment of its staining properties. It was found that $[Ru(dip)_2(bpy\text{-}2\text{-}nitroIm)]^{2+}$ quickly and easily accumulates in cancer cells. Even 1 h of incubation is sufficient to observe an efficient cell luminescence. The lengthening of incubation time from 4 to 24 h does not intensify the emission properties of the cells as

shown in Fig. 3. A linear correlation between the amount of incubated compound and the level of luminescence expressed by the cells observed in the concentration range 1-50 μM suggests that $[Ru(dip)_2(bpy\text{-}2\text{-}nitroIm)]^{2+}$ can easily and efficiently accumulate in the cells. At low concentration of dye (1 μM) the luminescence intensification relative to the blank has a value of ca. 20 for both incubation times, which is quite promising for its application in optical imaging. This value is at least two times higher compare to the compounds of type $[Ru(dip)_2(L)]^{2+}$ (where L is CH_3bpyCOOH, bpy$(COOH)_2$, dppz) [14, 50]. The presence of dip ligands facilitate the uptake of the complex, probably due to their lipophilicity, which helps in the passive crossing of the cell membrane.[14, 50] The detailed mechanism of uptake for these type of complexes is poorly understand and both the passive and active transports are suggested [50-52].

Fig. 3.

The excellent luminescent properties were further confirmed by the microscopy fluorescence imaging performed on the CT26 cells incubated with $[Ru(dip)_2(bpy\text{-}2\text{-}nitroIm)]^{2+}$ for 1 h (Fig. 4A). At concentration of 10 μM the compound is transported inside the cells and stains quite homogenously the cytoplasm as well as different organelles, which is seen by the local increase of luminescence intensity. These results are in good correlation with the observed increased in luminescence intensity of ruthenium compound after protein binding. Weak labeling in the nucleus compartment is observed, which can arise either from the weak interaction between ruthenium complex and nucleus DNA or the quenching of the ruthenium complex luminescence by intercalating. Lowering the complex concentration (5 μM) leads to staining only selected cells while further decrease of $[Ru(dip)_2(bpy\text{-}2\text{-}nitroIm)]^{2+}$ down to 1 μM causes differentiation in its accumulation in the cell. However the detailed

evaluation of its distribution within the cell is not possible due to too low magnification. The recent data for similar type of complexes ($[Ru(dip)_2(L)]^{2+}$, where L is CH_3bpyCOOH, bpy$(COOH)_2$, dppz) [14, 50] have also shown that nucleus compartment is rather weakly labelled.

Fig. 4.

The cytotoxic effect of the synthesized compound was tested using the standard MTT test. The $[Ru(dip)_2$(bpy-2-nitroIm)$]^{2+}$ was found to be quite cytotoxic with LD_{50} = 13 ± 3 μM measured after 4 h of incubation with cells (Fig. 5). The increase of exposure time up to 24 h does not influence the cytotoxicity, and this correlates very well with the observed lack of changes in the luminescence level. The nitroimidazole moiety alone exhibit rather weak toxicity (Fig. 5), therefore it can be assumed that the antiproliferative effect arise from ruthenium residue. The application of the studied compound as a dye in optical imaging is therefore limited to the concentration of 1 μM and lower, for which the growth inhibition is marginal. However at higher doses $[Ru(dip)_2$(bpy-2-nitroIm)$]^{2+}$ could be utilized as a cytotoxic agent enabling visualization of the field of action.

Fig. 5.

3.6. Preliminary in vitro studies under hypoxic conditions

Behavior of $[Ru(dip)_2$(bpy-NitroIm)$]^{2+}$ under hypoxic in relation to normoxic conditions was studied using human lung adenocarcinoma epithelial (A549) cell line. This cell line was selected because it is known to express nitroreductase[53], enzyme which can reduced the nitroimidazole moiety. The studied ruthenium complex exhibits dose-dependent

growth inhibitory effect on tested A549 cell line. The cytotoxicity of $[Ru(dip)_2(bpy\text{-}NitroIm)]^{2+}$ increased clearly under hypoxic conditions: LC_{50} decreased from 11.8 ± 1.2 μM under normoxic conditions to 7.7 ± 0.4 μM under 1% of oxygen. These results can be explained in terms of higher accumulation of ruthenium compound under hypoxic conditions or the involvement of additional mechanism of toxicity triggered by hypoxia.

The cellular uptake of $[Ru(dip)_2(bpy\text{-}NitroIm)]^{2+}$ was monitored directly by following the luminescent signal of treated cells using flow cytometry. It is known, that the stress triggered by hypoxic conditions results in worse growth as well as slower metabolism of cells compare to those under normoxia. Therefore, in order to appropriate evaluate the change in the uptake under both conditions, structurally similar compound $[Ru(dip)_2(bpy)]^{2+}$, was used as a reference. It is presume, that the uptake of $[Ru(dip)_2(bpy)]^{2+}$ is not directly dependent on hypoxic/normoxic conditions, so its accumulation (under normoxia and hypoxia) was applied as a base level of the uptake under corresponding conditions. The relative intensity of luminescence of cells treated with $[Ru(dip)_2(bpy\text{-}NitroIm)]^{2+}$ was calculated as a percentage of the luminescence intensity of cells incubated with $[Ru(dip)_2(bpy)]^{2+}$ at 2 μM concentration under the same conditions. As shown in Fig. 6, the relative luminescence intensity of cells incubated with $[Ru(dip)_2(bpy\text{-}NitroIm)]^{2+}$ under hypoxic conditions is always higher than for cells incubated under normoxic conditions. The difference is more pronounce with increased concentration of the studied compound. When studies are carried out in medium containing serum still the uptake of $[Ru(dip)_2(bpy\text{-}NitroIm)]^{2+}$ is higher under hypoxia, however a distinct decrease in accumulation of ruthenium complex is observed regardless of applied conditions. This points to formation of adducts between ruthenium complex and serum components (most probably albumin) which are not accessible for cells and therefore the accumulation of $[Ru(dip)_2(bpy\text{-}NitroIm)]^{2+}$ becomes lower.

Fig. 6.

To confirm the ability of new synthesized ruthenium complex to be "trapped" inside the cells under hypoxic conditions, the intensity of luminescence of treated cells was measured after one day of growth in ruthenium free medium. Retention factor was presented as a percentage of cells luminescence intensity compared to an original luminescence intensity of the cells measured directly after 24 h of the incubation with ruthenium complex. Results were compared with retention ability of $[Ru(dip)_2(bpy)]^{2+}$ for which the uptake and the loss is not expected to be related to hypoxic conditions. As shown in Table 1 $[Ru(dip)_2(bpy\text{-}NitroIm)]^{2+}$ preserves its luminescence in the cells up to 83–89% and this level is ca. 30% higher than found for $[Ru(dip)_2(bpy)]^{2+}$. The main difference between these two complexes arises from the presence of nitroimidazole moiety. Therefore, one can speculate that $[Ru(dip)_2(bpy\text{-}NitroIm)]^{2+}$ can be trapped inside the cells due to reduction of nitro group follow by its binding to biomolecules under hypoxic conditions.

Table 1.

4. Conclusions

The photophysical and biological properties of $[Ru(dip)_2(bpy\text{-}2\text{-}nitroIm)]^{2+}$ indicate that this compound has potential to be applied as optical imaging probe and cytotoxic agent. Preliminary results have shown that this compound is more toxic towards hypoxic tissues, exhibits higher accumulation inside hypoxic cells, which combined with higher luminescence parameters (quantum yield, luminescence lifetime) in deoxygenated atmosphere, makes reasonable assumption that it can be applied for detection of hypoxic tissues inside body. Our future work will focus on *in vitro/in vivo* studies toward verification its potential as a hypoxia marker. Such achievement would be of particular benefit since the assessment of hypoxia state is one of the most important parameter needed for estimation of cancer progress and choosing the appropriate treatment.

This dye can be also regarded as an alternative for pimonidazole, a currently exploring hypoxia marker, which administrated prior to surgery can help in identification of lower oxygen content [18]. As already mentioned, the visualization procedure involves application of a complicated immunochemical test, while for the studied compound irradiation with an appropriate light beam (around 450 nm) would most probably be sufficient. The intra-operative multispectral system has been already successfully tested for clinical use for folate and fluoresceine isothiocyanate conjugate [54]. Combination of two methods (fluorescence imaging during cytoreductive procedure) allowed 5-fold increase of tumor deposits detected by surgeons as well as making possible the excision of tumors of size < 1 mm. Using other types of optical probes, for example based on ruthenium complexes, could allow for application of these techniques in a wider range of surgery procedures.

5. Abbreviations

bpy	2,2’-bipyridine
bpy-2-nitroIm	4-[3-(2-nitro-1H-imidazol-1-yl)propyl]-2,2'-bipyridine
DMEM	Dulbecco's modified Eagle's medium
dip	4,7-diphenyl-1,10-phenanthroline
DME	dimethoxyethane
DMF	N, N-dimethylformamide
dppz	dipyrido[3,2-*a*:2’,3’-*c*]phenazine
EB	ethidium bromide
HSA	human serum albumin
HRMS	high resolution mass spectrometry
LC	liquid chromatography
LD_{50}	lethal dose, 50%

MLCT	metal to ligand charge transfer
MTT	3-(4,5-dimethylthiazol-2-yl)-2,5-diphenyltetrazolium bromide salt
NIR	near infrared
PBS	Phosphate buffered saline
PET	positron emission tomography
phen	1,10-phenanthroline
THF	tetrahydrofuran

Acknowledgments

Financial support from the National Science Center (grant no. N N204 247340) is acknowledged. The research was carried out with equipment purchased with financial support from the European Regional Development Fund within the framework of the Polish Innovation Economy Operational Program (contract no. POIG.0 2.01.00-12-0 23/08). O.M. acknowledges the financial support from the project Interdisciplinary PhD Studies "Molecular sciences for medicine" (co-financed by the European Social Fund within the Human Capital Operational Programme). M.M thanks for support from Bourses du Gouvernement Français. We thank Prof. A. Józkowicz for the access to hypoxia station.

References

[1] Y.J. Liu, N. Zhang, Biomaterials 33 (2012) 5363-5375.

[2] R. Bardhan, S. Lal, A. Joshi, N.J. Halas, Acc. Chem. Res. 44 (2011) 936-946.

[3] J.W. Dobrucki, J. Photochem. Photobiol. B-Biol. 65 (2001) 136-144.

[4] J.R. Lakowicz, Principles of Fluorescence Spectroscopy, Springer, New York, 2006, pp. 954.

[5] H. Komatsu, K. Yoshihara, H. Yamada, Y. Kimura, A. Son, S. Nishimoto, K. Tanabe, Chem. Eur. J. 19 (2013) 1971-1977.

[6] J.M. Brown, W.R. Wilson, Nat. Rev. Cancer 4 (2004) 437-447.

[7] Q.T. Le, D. Courter, Cancer Metastasis Rev. 27 (2008) 351-362.

[8] J.X. Zhang, J.W. Zhou, C.F. Chan, D.W.J. Kwong, H.L. Tam, N.K. Mak, K.L. Wong, W.K. Wong, BioConjugate Chem. 23 (2012) 1623-1638.

[9] M.J. Li, K.M.C. Wong, C. Yi, V.W.W. Yam, Chem. Eur. J. 18 (2012) 8727-8730.

[10] K.K.W. Lo, T.K.M. Lee, J.S.Y. Lau, W.L. Poon, S.H. Cheng, Inorg. Chem. 47 (2008) 200-208.

[11] F. Dosio, B. Stella, A. Ferrero, C. Garino, D. Zonari, S. Arpicco, L. Cattel, S. Giordano, R. Gobetto, Int. J. Pharm. 440 (2013) 221-228.

[12] C.A. Puckett, J.K. Barton, Bioorg. Med. Chem. 18 (2010) 3564-3569.

[13] C.A. Puckett, J.K. Barton, J. Am. Chem. Soc. 131 (2009) 8738-8739.

[14] M. Lamoureux, O. Seksek, J. Fluoresc. 20 (2010) 631-643.

[15] C.A. Puckett, J.K. Barton, J. Am. Chem. Soc. 129 (2007) 46-47.

[16] S. Kizaka-Kondoh, H. Konse-Nagasawa, Cancer Sci. 100 (2009) 1366-1373.

[17] M.A. Varia, D.P. Calkins-Adams, L.H. Rinker, A.S. Kennedy, D.B. Novotny, W.C. Fowler, J.A. Raleigh, Gynecologic Oncol. 71 (1998) 270-277.

[18] http://clinicaltrials.gov/ct2/show/NCT01248637, 22.10 (2012).

[19] P.D. Bonnitcha, S.R. Bayly, M.B.M. Theobald, H.M. Betts, J.S. Lewis, J.R. Dilworth, J. Inorg. Biochem. 104 (2010) 126-135.

[20] E.L. Engelhardt, R.F. Schneider, S.H. Seeholzer, C.C. Stobbe, J.D. Chapman, J. Nucl. Med. 43 (2002) 837-850.

[21] N.K. Wagh, Z.Y. Zhou, S.M. Ogbomo, W. Shi, S.K. Brusnahan, J.C. Garrison, Bioconjgate Chem. 23 (2012) 527-537.

[22] F.A. Rojas-Quijano, G. Tircso, E.T. Benyo, Z. Baranyai, H.T. Hoang, F.K. Kalman, P.K. Gulaka, V.D. Kodibagkar, S. Aime, Z. Kovacs, A.D. Sherry, Chem. Eur. J. 18 (2012) 9669-9676.

[23] K. Okuda, Y. Okabe, T. Kadonosono, T. Ueno, B.G.M. Youssif, S. Kizaka-Kondoh, H. Nagasawa, Bioconjgate Chem. 23 (2012) 324-329.

[24] N.C. Biswal, C. Pavlik, M.B. Smith, A. Aguirre, Y. Xu, S. Zanganeh, L.T. Kuhn, K.P. Claffey, Q. Zhu, J. Biomed. Opt. 16 (2011) 066001-066008.

[25] D.A.M. Egbe, A.M. Amer, E. Klemm, Des. Monomers Polym. 4 (2001) 169-175.

[26] R. Caspar, C. Cordier, J.B. Waern, C. Guyard-Duhayon, M. Gruselle, P. Le Floch, H. Amouri, Inorg. Chem. 45 (2006) 4071-4078.

[27] J.B. Waern, C. Desmarets, L. Chamoreau, H. Amouri, A. Barbieri, C. Sabatini, B. Ventura, F. Barigelletti, Inorg. Chem. 47 (2008) 3340-3348.

[28] R.B. Nair, B.M. Cullum, C.J. Murphy, Inorg. Chem. 36 (1997) 962-965.

[29] F.N. Castellano, J.D. Dattelbaum, J.R. Lakowicz, Anal. Biochem. 255 (1998) 165-170.

[30] O. Mazuryk, E. Niemiec, G. Stochel, I. Gillaizeau, M. Brindell, J. Lumin. 140 (2013) 51-56.

[31] J. Weyermanna, D. Lochmanna, Z. A., Int. J. Pharm. 288 (2005) 369-376.

[32] J.S. Bair, R.G. Harrison, J. Org. Chem. 72 (2007) 6653-6661.

[33] D. Wenkert, R.B. Woodward, J. Org. Chem. 48 (1983) 283-289.

[34] A. Juris, V. Balzani, F. Barigelletti, S. Campagna, P. Belser, A. Vonzelewsky, Coord. Chem. Rev. 84 (1988) 85-277.

[35] Y. Liu, Q. Yu, C. Wang, D. Sun, Y. Huang, Y. Zhou, J. Liu, Inorg. Chem. Comm. 24 (2012) 104-109.

[36] Y. Liu, Y. Xu, X. Qian, J. Liu, L. Shen, J. Lic, Y. Zhang, Bioorg. Med. Chem. 14 (2006) 2935–2941.

[37] A. Srishailam, Y.R. Kumar, N.M.D. Gabra, P.V. Reddy, N. Deepika, N. Veerababu, S. Satyanarayanna, J. Fluoresc. 23 (2013) 897-908.

[38] B. Sun, Y.C. Wang, C. Qian, J. Chu, S.M. Liang, H. Chao, L.N. Ji, J. Mol. Struct. 963 (2010) 153-159.

[39] X.W. Liu, S.B. Zhang, L. Li, Y.D. Chen, J.L. Lu, J. Organomet. Chem 729 (2013) 1-8.

[40] L. Blackmore, R. Moriarty, C. Dolan, K. Adamson, R.J. Forster, M. Devocelle, T.E. Keyes, Chem. Commun. 49 (2013) 2658-2660.

[41] C. Wang, Q. Yu, L. Yang, Y. Liu, D. Sun, Y. Huang, Y. Zhou, Q. Zhang, J. Liu, Biometals 26 (2013) 387-402.

[42] L. Strekowski, B. Wilson, Mut. Res. 623 (2007) 3-13.
[43] M.R. Gill, H. Derrat, C.G.W. Smythe, G. Battaglia, J.A. Thomas, ChemBioChem 12 (2011) 877-880.
[44] A.P. Minton, J. Biol. Chem. 276 (2001) 10577-10580.
[45] X.W. Liu, Z.G. Chen, L. Li, Y.D. Chen, J.L. Lu, D.S. Zhang, Spectrochim. Acta Mol. Biomol. Spectrosc. 102 (2013) 142-149.
[46] A.J. McConnell, M.H. Lim, E.D. Olmon, H. Song, E. Dervan, J.K. Barton, Inorg. Chem. 51 (2012) 12511-12520.
[47] W.R. Glomm, S. Volden, J. Sjoblom, M. Lindgren, Chem. Mater. 17 (2005) 5512-5520.
[48] P.U. Maheswari, V. Rajendiran, M. Palaniandavar, R. Thomas, G.U. Kulkarni, Inorg. Chim. Acta 359 (2006) 4601-4612.
[49] F. Gao, H. Chao, F. Zhou, Y.X. Yuan, B. Peng, L.N. Ji, J. Inorg. Biochem. 100 (2006) 1487-1494.
[50] C.A. Puckett, J.K. Barton, Biochemistry 47 (2008) 11711–11716.
[51] F.R. Svensson, J. Andersson, H.L. Amand, P. Lincoln, J. Biol. Inorg. Chem. 17 (2012) 565-571.
[52] C.A. Puckett, J.R. Ernst, J.K. Barton, Dalton Trans. 39 (2010) 1159 - 1170.
[53] Z. Li, X.H. Li, X.H. Gao, Y.Y. Zhang, W. Shi, H.M. Ma, Anal. Chem. 85 (2013) 3926-3932.
[54] G.M. van Dam, G. Themelis, L.M.A. Crane, N.J. Harlaar, R.G. Pleijhuis, W. Kelder, A. Sarantopoulos, J.S. de Jong, H.J.G. Arts, A.G.J. van der Zee, J. Bart, P.S. Low, V.

Schemes and Figures Captions

Scheme 1. $[Ru(dip)_2(bpy\text{-}2\text{-}nitroIm)]^{2+}$

Scheme 2. The synthetic pathway for the bpy-2-nitroIm (**8**) ligand.

Fig. 1. Absorption (A) and emission spectra (E) (excitation at 463 nm) of $[Ru(dip)_2(bpy\text{-}2\text{-}nitroIm)]^{2+}$ in H_2O.

Fig. 2. Luminescence quantum yield (■) and average lifetime (●) of ruthenium complex for different [HSA]/[Ru] ratios. Experimental conditions: [HSA] = 1 μM, [Ru]= 1-3 μM; PBS pH 7.4.

Fig. 3. Luminescence intensity of seeded CT26 cells measured after incubation with $[Ru(dip)_2(bpy\text{-}2\text{-}nitroIm)]^{2+}$ during 4 (■) and 24 h (●) monitored at 621 nm upon excitation at 463 nm, [CT26] = 30×10^3 cell/well.

Fig. 4. Fluorescent (A) and the corresponding bright-field (B) microscopic images of CT26 cells treated with $[Ru(dip)_2(bpy\text{-}2\text{-}nitroIm)]^{2+}$. Experimental conditions: [CT26] = 300×10^3 cell/well; [Ru] = 10×10^{-6} M.

Fig. 5. Cytotoxic effect of $[Ru(dip)_2(bpy\text{-}2\text{-}nitroIm)]^{2+}$ (●) and bpy-2-nitroIm (■) on CT26 cell after incubation during 4 h. Cell viability was assessed by MTT assay.

Fig. 6. Relative luminescence intensity of A549 cells incubated with $[Ru(dip)_2(bpy\text{-}NitroIm)]^{2+}$ in medium without (S-) or with (S+, 2%) serum under normoxic and hypoxic conditions.

Table 1. Retention of ruthenium complexes in A549 cells under hypoxic conditions estimated by the monitoring of luminescence intensity conserved inside the cells cultivated for 24 h in medium (2% FBS) without addition of these complexes.

Concentration [μM]	$[Ru(dip)_2(bpy\text{-}NitroIm)]^{2+}$	$[Ru(dip)_2(bpy)]^{2+}$
2	83 %	57 %
4	85 %	53 %
6	89 %	63 %

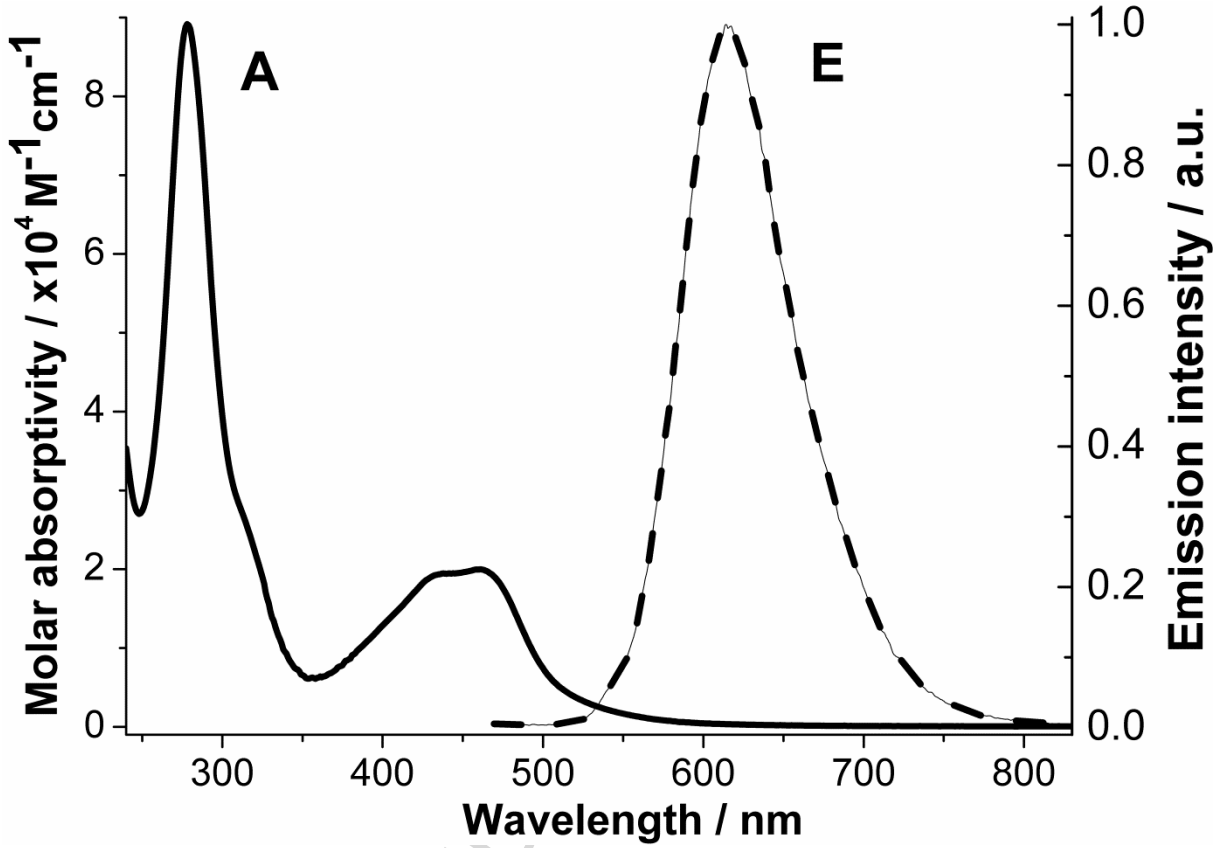

Figure 1

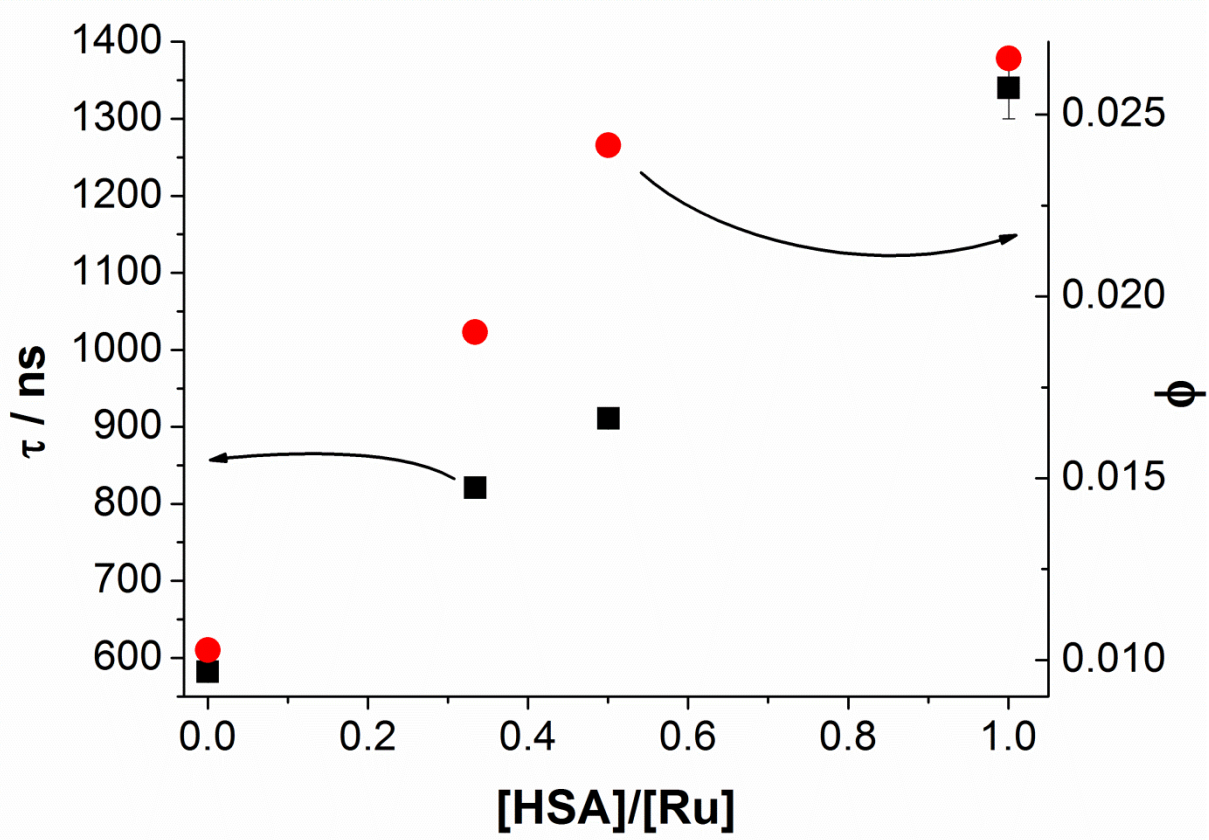

Figure 2

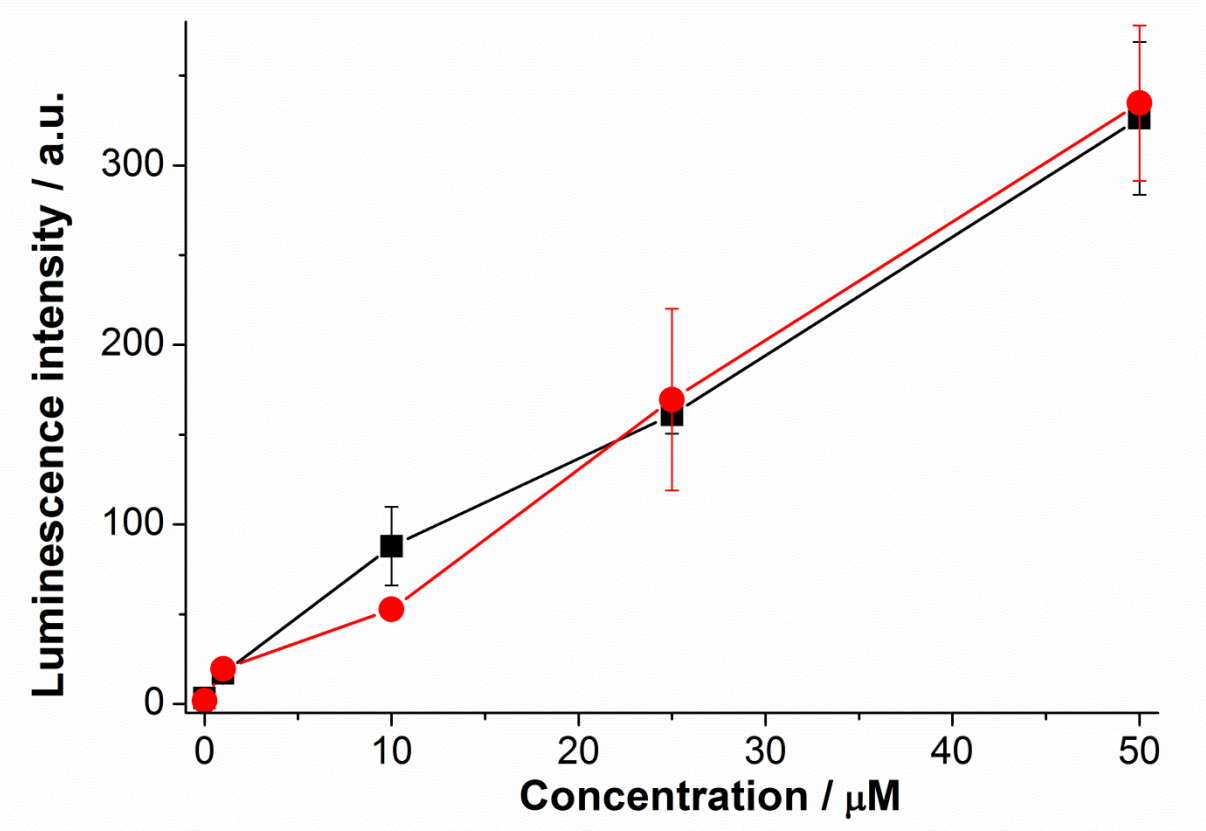

Figure 3

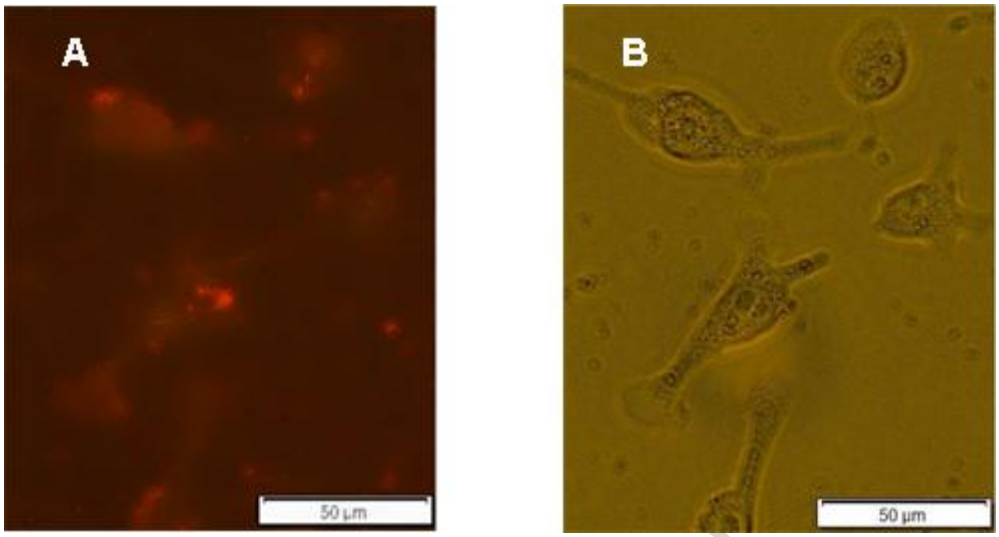

Figure 4

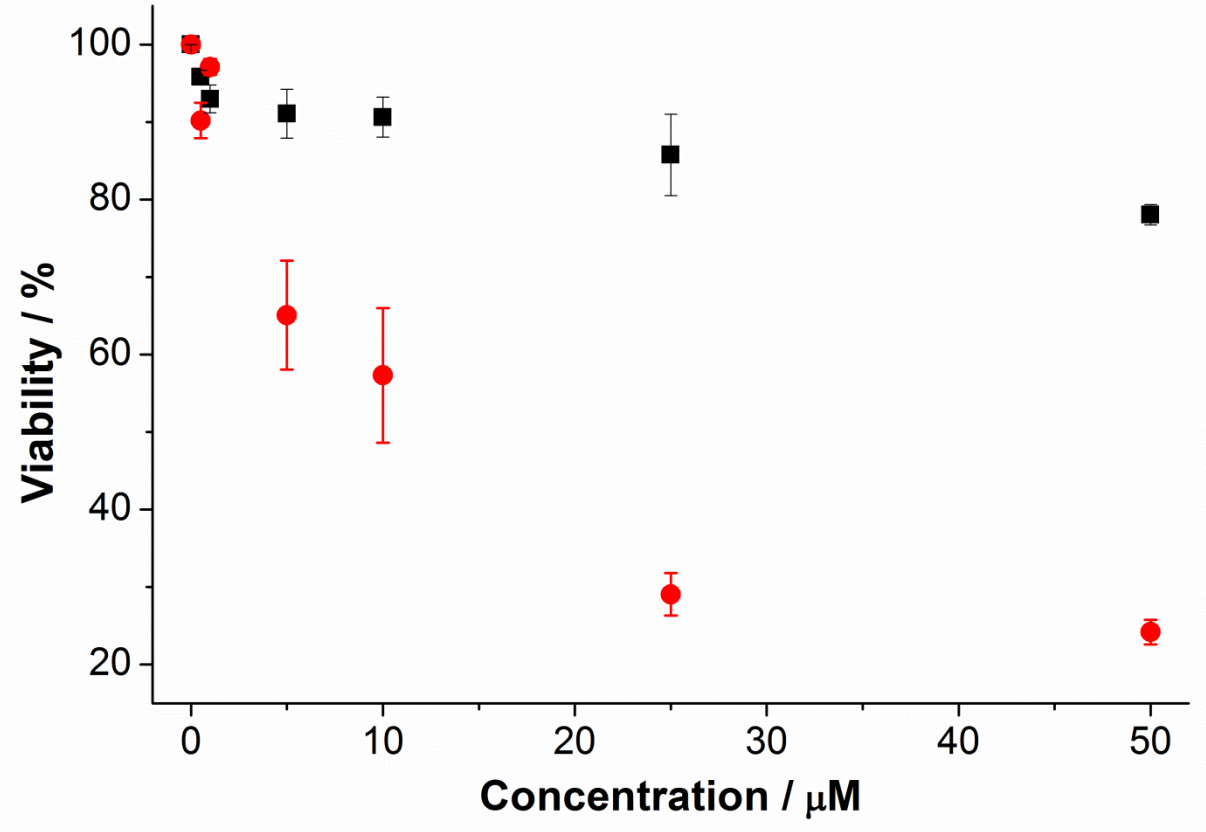

Figure 5

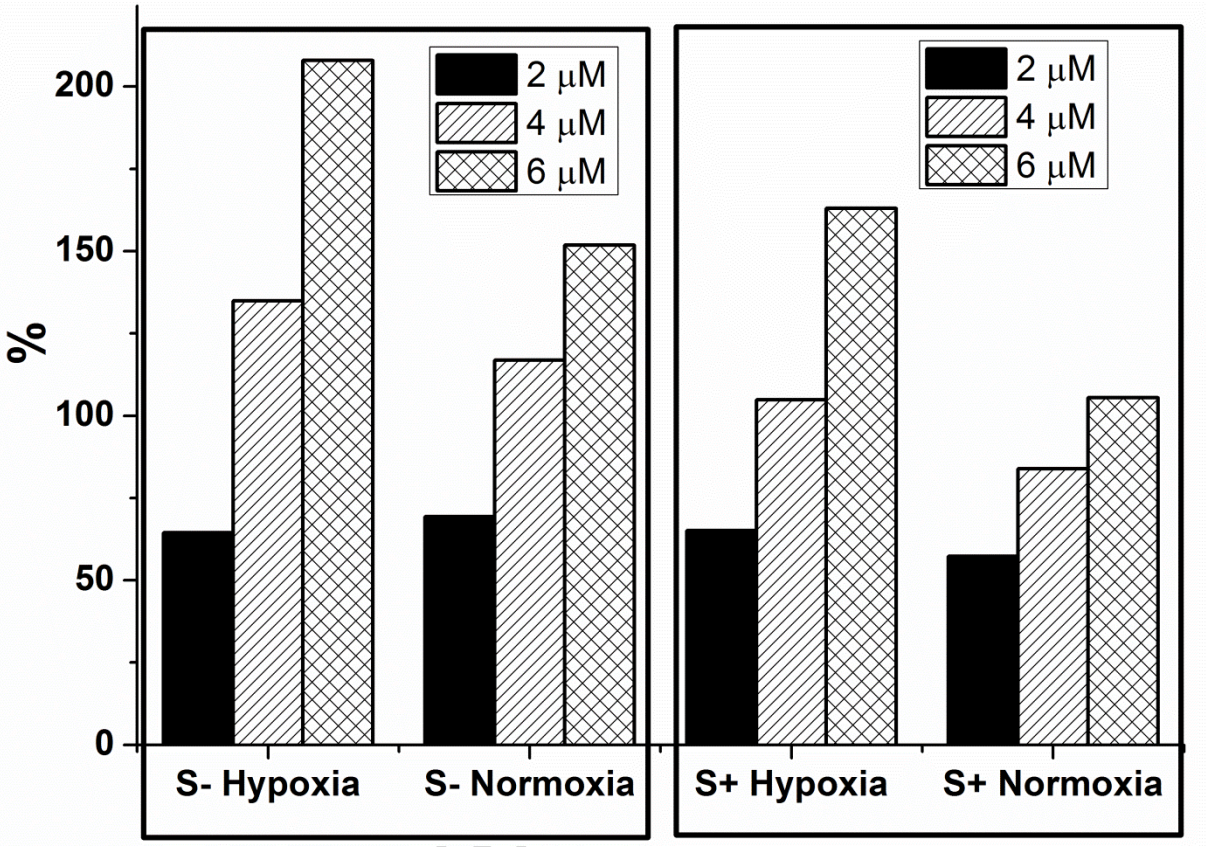

Figure 6

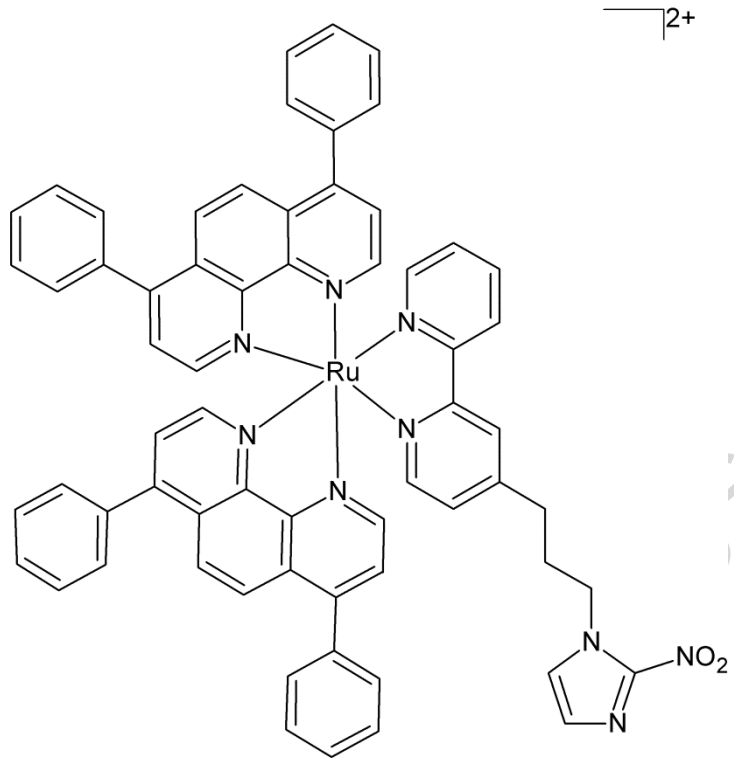

Scheme 1

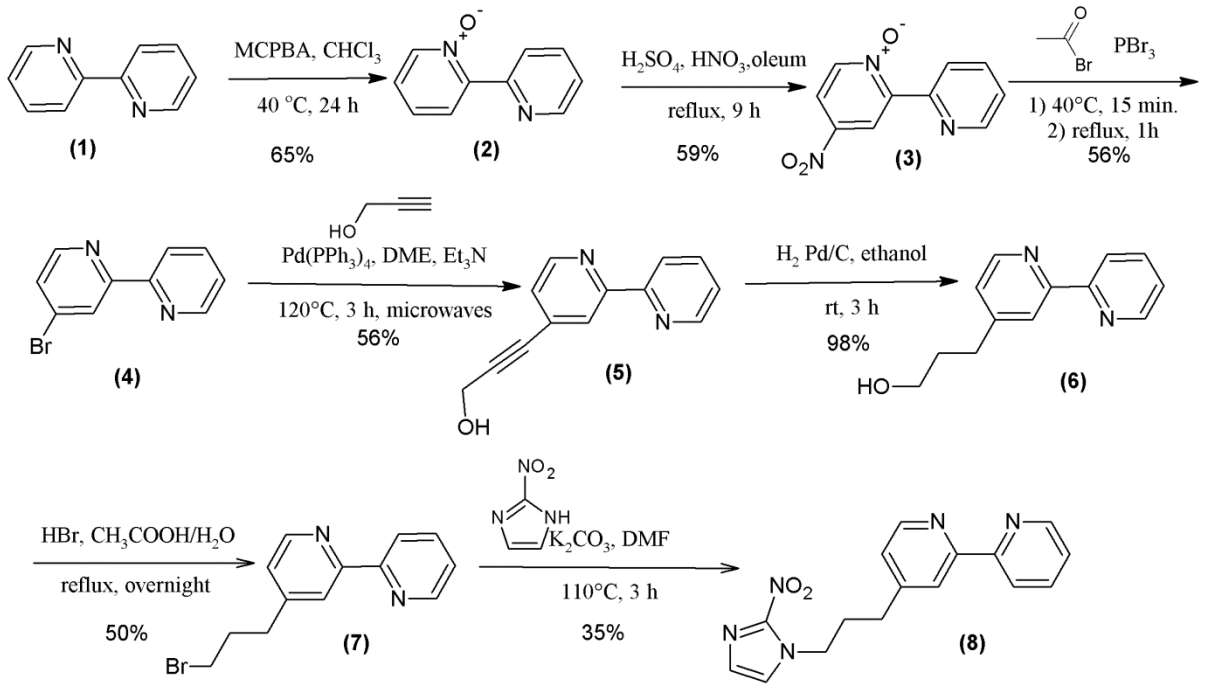

Scheme 2

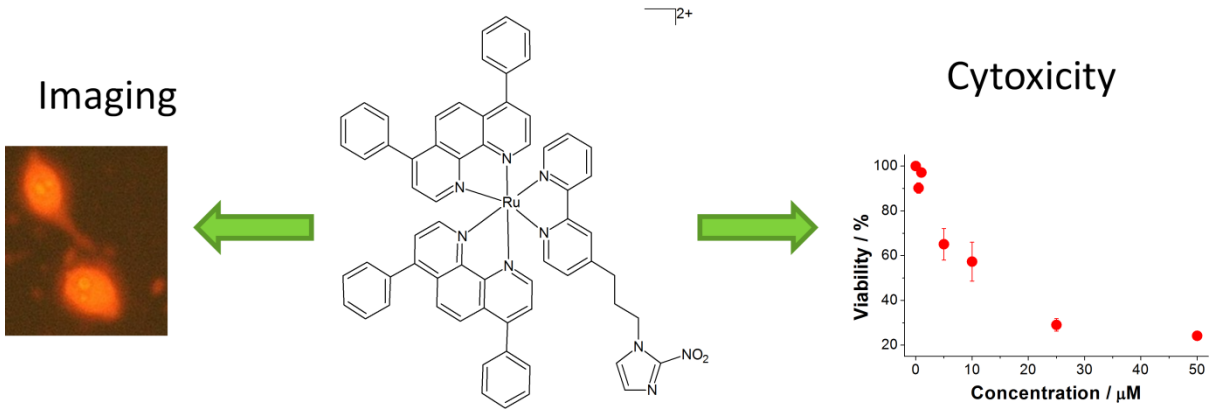

Graphical abstract

Highlights

- Ru polypyridyl complex with 2-nitroimidazole moiety is a potential theranostic agent.
- Luminescence properties of Ru complex are markedly increased in oxygen-free solution.
- The interaction of Ru complex with albumin enhances its luminescence properties.
- Luminescence expressed by cells linearly increases with applied Ru concentration.
- Ru complex is quite cytotoxic with LD_{50} of 10 μM.